

MTL TR 92-56

AD-A257 498



2

# ADHESION AND CORROSION BEHAVIOR OF Al-Zn AND TiN/Ti/TiN COATINGS ON A DU-0.75 WT% ALLOY

DTIC  
ELECTE  
NOV 30 1992  
S C D

F. C. CHANG, M. LEVY, R. HUIE, M. KANE, and  
P. BUCKLEY

U.S. ARMY MATERIALS TECHNOLOGY LABORATORY  
METALS RESEARCH BRANCH

Z. KATTAMIS

UNIVERSITY OF CONNETICUT  
STORRS, CT

G. R. LAKSHMINARAYAN

U.S. ARMAMENT RESEARCH, DEVELOPMENT, AND ENGINEERING CENTER  
PICATINNY ARSENAL, NJ

P48

92-30344

August 1992

Approved for public release; distribution unlimited.



US ARMY  
LABORATORY COMMAND  
MATERIALS TECHNOLOGY LABORATORY



U.S. ARMY MATERIALS TECHNOLOGY LABORATORY  
Watertown, Massachusetts 02172-0001

The findings in this report are not to be construed as an official Department of the Army position, unless so designated by other authorized documents.

Mention of any trade names or manufacturers in this report shall not be construed as advertising nor as an official indorsement or approval of such products or companies by the United States Government.

#### DISPOSITION INSTRUCTIONS

Destroy this report when it is no longer needed.  
Do not return it to the originator.

**SECURITY CLASSIFICATION OF THIS PAGE (When Data Entered)**

REPORT DOCUMENTATION PAGE		READ INSTRUCTIONS BEFORE COMPLETING FORM	
1. REPORT NUMBER MTL TR 92-56		2. GOVT ACCESSION NO.	
3. RECIPIENT'S CATALOG NUMBER		4. TITLE (and Subtitle) ADHESION AND CORROSION BEHAVIOR OF Al-Zn AND TiN/Ti/TiN COATINGS ON A DU-0.75wt% Ti ALLOY	
5. TYPE OF REPORT & PERIOD COVERED		6. PERFORMING ORG. REPORT NUMBER	
7. AUTHOR(s) F. C. Chang, M. Levy, R. Huie, M. Kane, P. Buckley, T. Z. Kattamis,* and G. R. Lakshminarayan†		8. CONTRACT OR GRANT NUMBER(s)	
9. PERFORMING ORGANIZATION NAME AND ADDRESS U.S. Army Materials Technology Laboratory Watertown, Massachusetts 02172-0001 ATTN: SLCMT-EMM		10. PROGRAM ELEMENT, PROJECT, TASK AREA & WORK UNIT NUMBERS	
11. CONTROLLING OFFICE NAME AND ADDRESS U.S. Army Laboratory Command 2800 Powder Mill Road Adelphi, Maryland 20783-1145		12. REPORT DATE August 1992	
13. NUMBER OF PAGES 12		14. MONITORING AGENCY NAME & ADDRESS (if different from Controlling Office)	
15. SECURITY CLASS. (of this report)  Unclassified		15a. DECLASSIFICATION/DOWNGRADING SCHEDULE	
16. DISTRIBUTION STATEMENT (of this Report)  Approved for public release; distribution unlimited.			
17. DISTRIBUTION STATEMENT (of the abstract entered in Block 20, if different from Report)			
18. SUPPLEMENTARY NOTES  *Dept. of Metallurgy, Univ. of Connecticut, Storrs, CT †U.S. Armament RD&E Center, Picatinny Arsenal, NJ (SEE REVERSE)			
19. KEY WORDS (Continue on reverse side if necessary and identify by block number) Uranium alloys Uranium-titanium alloys Vapor deposition Corrosion resistance Mechanical properties Scanning electron microscopy			
20. ABSTRACT (Continue on reverse side if necessary and identify by block number)  (SEE REVERSE SIDE)			

Block No. 18. continued

Presented at Proceedings of the 1991 International Conference on Metallurgical Coatings and Thin Films. Published in Surface and Coatings Technology, 49 (1991) 87-96.

Block No. 20

## ABSTRACT.

Al-Zn alloy and multilayer TiN/Ti/TiN thin coatings were deposited on DU-0.75Ti alloy specimens by a cathodic arc plasma physical vapor deposition process. The quality, soundness and adhesion of the coatings to the substrate were evaluated by automatic scratch testing, in combination with optical and scanning electron microscopy examination of the scratch morphology. The galvanic corrosion behavior of DU-0.75Ti alloy coupled to the coated alloys and aluminum alloy 7075-T6 was also investigated by electrochemical tests in a 0.5 N NaCl aqueous solution.

# Adhesion and corrosion behavior of Al–Zn and TiN/Ti/TiN coatings on a DU–0.75wt.% Ti alloy

F. C. Chang, M. Levy, R. Huie, M. Kane and P. Buckley

U.S. Army Materials Technology Laboratory, Watertown, MA 02172-0001 (U.S.A.)

T. Z. Kattamis

Department of Metallurgy, University of Connecticut, Storrs, CT 06269-3136 (U.S.A.)

G. R. Lakshminarayan

U.S. Armament Research, Development and Engineering Center, Picatinny Arsenal, NJ 07806 (U.S.A.)

## Abstract

Al–Zn alloy and multilayer TiN/Ti/TiN thin coatings were deposited on DU–0.75Ti alloy specimens by a cathodic arc plasma physical vapor deposition process. The quality, soundness and adhesion of the coatings to the substrate were evaluated by automatic scratch testing, in combination with optical and scanning electron microscopy examination of the scratch morphology. The galvanic corrosion behavior of DU–0.75Ti alloy coupled to the coated alloys and aluminum alloy 7075-T6 was also investigated by electrochemical tests in a 0.5 N NaCl aqueous solution.

## 1. Introduction

In a previous study [1] of various coatings deposited on DU–0.75Ti alloy (where DU means depleted uranium and where the composition is in weight per cent) by a cathodic arc plasma physical vapor deposition (PVD) process using elemental targets, Al–Zn coatings were found to be anodic (sacrificial) with useful life governed by their thickness and integrity. Titanium and TiN coatings, on the contrary, were found to be cathodic; hence to be effective they must be defect free. Surface morphology studies by scanning electron microscopy (SEM), as well as electrochemical polarization and long-term immersion tests in aerated 3.5 wt.% NaCl aqueous solution indicated that Al–Zn alloy is the best of four metallic sacrificial coatings tested for improving the corrosion resistance of DU–0.75Ti. In a subsequent evaluation [2] of the adhesion, soundness and comparative quality of various coatings by automatic scratch testing in combination with optical and SEM observations of the scratch and the adjacent coating surface, it was concluded that (1) alloyed metallic coatings, Al–Zn and Al–Mg, on DU–0.75Ti specimens exhibit higher cohesive and adhesive (critical) loads than do elemental coatings, such as aluminum, zinc, magnesium and titanium (these anodic coatings adhere well to the substrate and offer excellent protection) and (2) TiN and the dual-layer Al/TiN coatings also exhibit good cohesion and adherence to the substrate (however, unless such cathodic coatings are defect free they will perform rather poorly).

The relative mechanical strength of coatings and of the coating–substrate interfaces may be conveniently evaluated by scratch testing. This procedure consists of progressively straining the substrate by deforming the coating–substrate interface with a diamond indenter and evaluating the cohesive load  $L_c$ , which is the minimum load required for crack initiation within the coating, as well as the adhesive load  $L_a$ , which is the minimum load at which the coating is detached from the substrate [3–7]. The interpretation of the critical loads for coating cohesion and adhesion has been analyzed by Steinmann *et al.* [8] and applied previously to similar systems [2].

The aim of the present investigation was to evaluate further the quality, soundness, adherence and the galvanic corrosion behavior of the two most promising coatings: Al–Zn alloy and multilayer TiN/Ti/TiN on DU–0.75Ti specimens. The cohesive and adhesive loads were determined using an automatic scratch testing apparatus, in combination with microscopic observations of the scratch and the adjacent coating surface. The galvanic corrosion behavior was evaluated by electrochemical tests in a 0.5 N NaCl aqueous solution in combination with microscopic examination of corroded surfaces.

## 2. Experimental procedure

### 2.1. Specimen preparation

Disk specimens of DU–0.75Ti, 25.40 or 15.89 mm in diameter, and 6.35 or 3.18 mm thick respectively, were

prepared and coated by Nuclear Metals, Concord, MA, using the cathodic arc plasma (PVD) process in a Multi-Arc Vacuum System (Multi-Arc Vacuum Systems, St. Paul, MN), as previously described [2]. Whereas in the previous study [2] elemental aluminum and zinc cathodes were used, the present study used pre-alloyed Al-45wt.% Zn targets (supplied by Bethlehem Steel Corporation, Bethlehem, PA). Higher zinc evaporation rates make control of the coating composition rather difficult. Coated specimens 25.40 mm in diameter in the as-received condition were used for automatic scratch testing.

The galvanic corrosion behavior of DU-0.75Ti coupled to the following alloys was studied: aluminum alloy 7075, DU-0.75Ti coated with an Al-Zn alloy, and DU-0.75Ti coated with a multilayered system consisting of an inner TiN layer, an intermediate titanium layer and an outer TiN layer. These specimens were machined into disks with a diameter of 15.89 mm and thickness of 3.18 mm. The uncoated DU and aluminum alloys were ground and polished using 600 grit silicon carbide paper to a surface roughness of about 0.25  $\mu\text{m}$  r.m.s. After coating, the DU disks were tested in the as-received condition. All specimens were degreased in acetone, followed by a methanol rinse and air dried prior to electrochemical corrosion testing in a 0.5 N NaCl solution at room temperature.

### 2.2. Specimen testing

The soundness and quality of 25.40 mm diameter coated specimens were evaluated primarily with a CSEM-Revetest (Centre Suisse d'Electronique et de Microtechnique, CSEM, CH-2007, Neuchâtel, Switzerland) automatic scratch testing apparatus. The original tip radius of the diamond indenter was 200  $\mu\text{m}$ . The apparatus and testing procedure have been described elsewhere [2, 7]. In all tests the sample table translation speed was 10 mm min<sup>-1</sup> with a loading rate of 100 N min<sup>-1</sup>; hence  $dL/dx = 10 \text{ N mm}^{-1}$ . The acoustic emission (AE) signal intensity, the frictional force  $F_f$  and the friction coefficient  $\mu^*$  were plotted vs. applied normal load  $F_n$ . The scratch track and coating surface morphology in the vicinity of the scratch were examined by optical microscopy and SEM.

Galvanic coupling was accomplished by an electrical short circuit between the sample electrodes 5 cm apart. A PAR model 273 system, functioning as a zero-resistance ammeter measured galvanic currents continuously as a function of time. The galvanic corrosion cell was instrumented so that a positive current density indicated that the DU-0.75Ti alloy was cathodic; conversely a negative value indicated anodic behavior. The exposed areas of each anode and cathode pair were the same. Post-test SEM examination and energy-dispersive

spectroscopy (EDS) analyses were performed for evidence of corrosion.

Anodic and cathodic potentiodynamic polarization scans of the each uncoupled specimen combination were made to complement the galvanic coupling data. The intersection of the anodic segment of the alloy behaving as the anode of a couple and the cathodic segment of the alloy behaving as cathode represented the potential and current density generated by that couple. The PAR potentiostat-galvanostat model 273 in conjunction with a PAR Softcorr 342 program was used for the potentiodynamic polarization scans. A scan rate of 0.3 mV s<sup>-1</sup> beginning at  $E_{\text{corr}}$  was used with a reference saturated calomel electrode (SCE), and two high density non-permeable graphite rod counterelectrodes; a PAR standard flat specimen holder model K105 with a sealing knife edge washed of Teflon exposed 1 cm<sup>2</sup> of specimen area to the test solution. Measurements began after immersion for 1 h to allow specimens to stabilize.

## 3. Results and discussion

### 3.1. Quality, soundness and adhesion of the coatings

#### 3.1.1. (Al-Zn)-coated DU-0.75Ti specimens

The coating thickness is fairly uniform with an average value of 8.33  $\mu\text{m}$ , as measured optically from transverse sections (Fig. 1(a)). The surface morphology, (Figs 1(c)-1(e)) consists of an agglomeration of spheroidal or flattened particles of a wide size distribution between about 1 and 35  $\mu\text{m}$ . Defects such as pits and micropores are also observed.

The variation in AE intensity,  $F_f$  and  $\mu^*$  vs. applied normal load  $F_n$  between 0 and 80 N is illustrated in Fig. 2. For this particular scratch a cohesive load  $L_c = 38.2 \text{ N}$ , and adhesive (critical) load  $L_a = 70.4 \text{ N}$  and an average friction coefficient  $\mu^* = 0.41$  were measured. Average values of  $L_c = 43.72 \text{ N}$  and  $L_a = 68.64 \text{ N}$  were determined (Table 1), using five scratches on two specimens 25.4 mm in diameter.

With increasing load the coating deforms plastically and the surface particles in the track gradually merge into a single mass (Fig. 1(c)). The first microcracks within the coating are observed at a load of about 37.9 N near the edges of the track (Fig. 1(d)). These transverse, presumably tensile microcracks form at a load of about 40 N and appear to be parallel to the trailing edge of the moving stylus. Longitudinal striations are observed all along the track within the coating and toward the end of the scratch within the substrate. Similar observations may be seen in Fig. 1(e) where a secondary system of very fine microcracks exists at the edges of the scratch in addition to the primary system within the track. Coating debris appears to be smeared on the sides of the track.

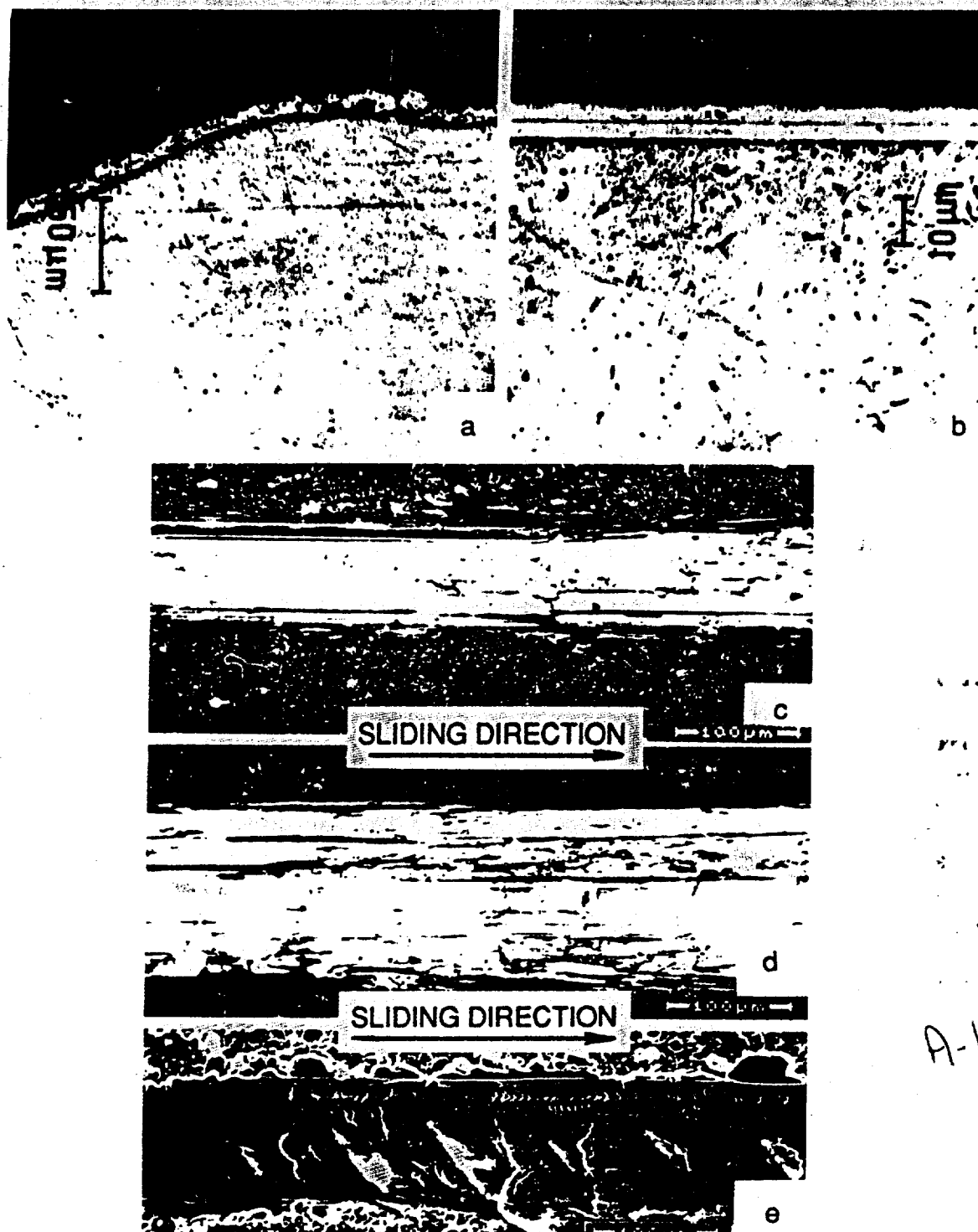


Fig. 1. Optical micrographs of transverse sections of (a) Al-Zn-coated and (b) multilayer TiN-Ti-TiN-coated DL-0.75Ti specimens (c) (d) optical micrographs of a scratch on Al-Zn-coated DL-0.75Ti specimens corresponding to normal loads of about (c) 37.6 N and (d) 42.1 N. (e) SEM micrograph of the same scratch corresponding to a normal load of 42 N. (Magnifications: (a) 300 $\times$ , (b) 750 $\times$ , (c) (d) 200 $\times$ .)

### 3.1.2. Multilayer (TiN-Ti-TiN)-coated DL-0.75Ti specimens

This coating consists of three layers with respective optically measured nominal thicknesses of 3 μm, 2 μm and 3 μm. Figure 1(b) illustrates the uniformity of

coating thickness. The upper TiN layer surface (Figs 3(a) and (b)) is relatively smooth with some occasional microscratches, fine TiN droplets and microcavities most probably caused by extraction of surface particles during handling or cleaning.

A-1 20

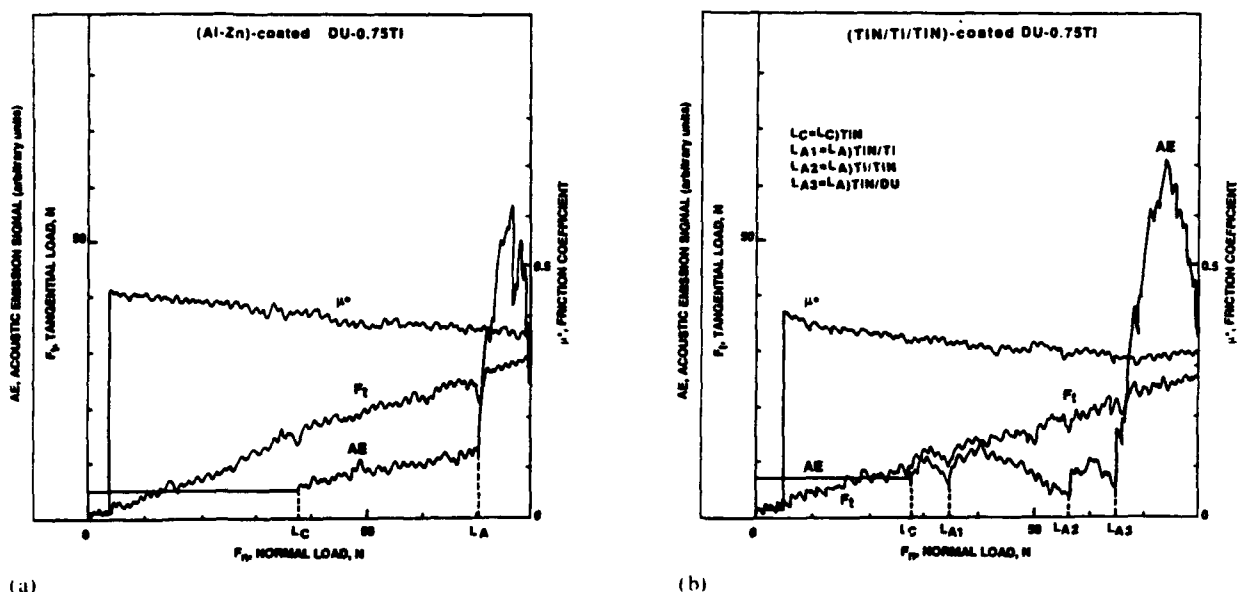


Fig. 2. AE signal intensity, frictional force  $F_t$  and friction coefficient  $\mu^*$  vs. normal load  $F_n$  between 0 and 80 N for (a) (Al-Zn)-coated and (b) multilayer TiN/Ti/TiN-coated DU-0.75Ti specimens.

TABLE 1. Average cohesive load,  $L_c$ , adhesive (critical) load  $L_A$  and friction coefficient  $\mu^*$

(TiN/Ti/TiN)-coated DU-0.75Ti	
$L_c (\equiv L_{c(TiN)})$	27.18 N
$L_{A1} (\equiv L_{A(TiN/Ti)})$	32.55 N
$L_{A2} (\equiv L_{A(Ti/TiN)})$	52.17 N
$L_{A3} (\equiv L_{A(TiN/DU-0.75Ti)})$	62.73 N
$\mu^*$	0.34
(Al-Zn)-coated DU-0.75Ti	
$L_c$	43.72 N
$L_A$	68.64 N
$\mu^*$	0.41

Typical AE,  $F_t$  and  $\mu^*$  curves vs.  $F_n$  between 0 and 80 N are illustrated in Fig. 2(b). For this particular scratch the shape characteristics of AE and to a lesser extent  $F_t$  indicate that crack initiation within the upper TiN layer occurs at  $L_c = 27.5$  N. The crack reaches the interface between the upper TiN and titanium layers, causing delamination at a load of  $L_{A1} = 34.5$  N. It subsequently propagates through the titanium layer, reaching the Ti-lower TiN layer interface and causing delamination at a load  $L_{A2} = 56.7$  N. Finally, the crack reaches the interface between the lower TiN layer and the substrate and causes delamination at the critical load,  $L_{A3} = 64.9$  N. Metallographic observations using the golden color of TiN and silvery color of titanium confirmed this interpretation of these measurements.

For the scratch in Fig. 2(b) the average  $\mu^*$  was 0.34. Average values using six scratches are given in Table 1.

TiN debris and islands of exposed titanium middle layer are illustrated in Fig. 3. In addition to longitudinal striations, very fine transverse microcracks, parallel to the trailing edge of the stylus and presumably tensile, are observed in the scratch.

Comparison of the two coatings (Table 1) clearly shows that (1) the cohesive load of the Al-Zn alloy coating is noticeably higher than that of the upper TiN layer in the multilayer TiN/Ti/TiN coating; and (2) the critical or adhesive load of Al-Zn on DU-0.75Ti is also slightly higher than that of the multilayer coating. For these tests all intrinsic parameters [2, 7, 8] that can affect the critical load values were kept constant ( $dL/dx = 10 \text{ N min}^{-1}$  and the stylus tip radius of 200  $\mu\text{m}$  with not much tip wear during testing of this batch of specimens). For the extrinsic parameters of substrate hardness and roughness, prior to coating there were no differences since all the substrate disks were sectioned from the same rod using the same procedure. Also, the coating thickness was roughly the same. However, the coating roughnesses, and thus the frictional forces and the friction coefficients, were not the same. It would therefore be speculative to generalize that Al-Zn coatings adhere better to the substrate than do the multilayer TiN/Ti/TiN coatings. None the less, in the latter the three layers delaminate from each other at substantially lower loads. Thus it appears that, for the set of process variable values used, the Al-Zn coating is mechanically superior to the multilayer TiN/Ti/TiN coating.



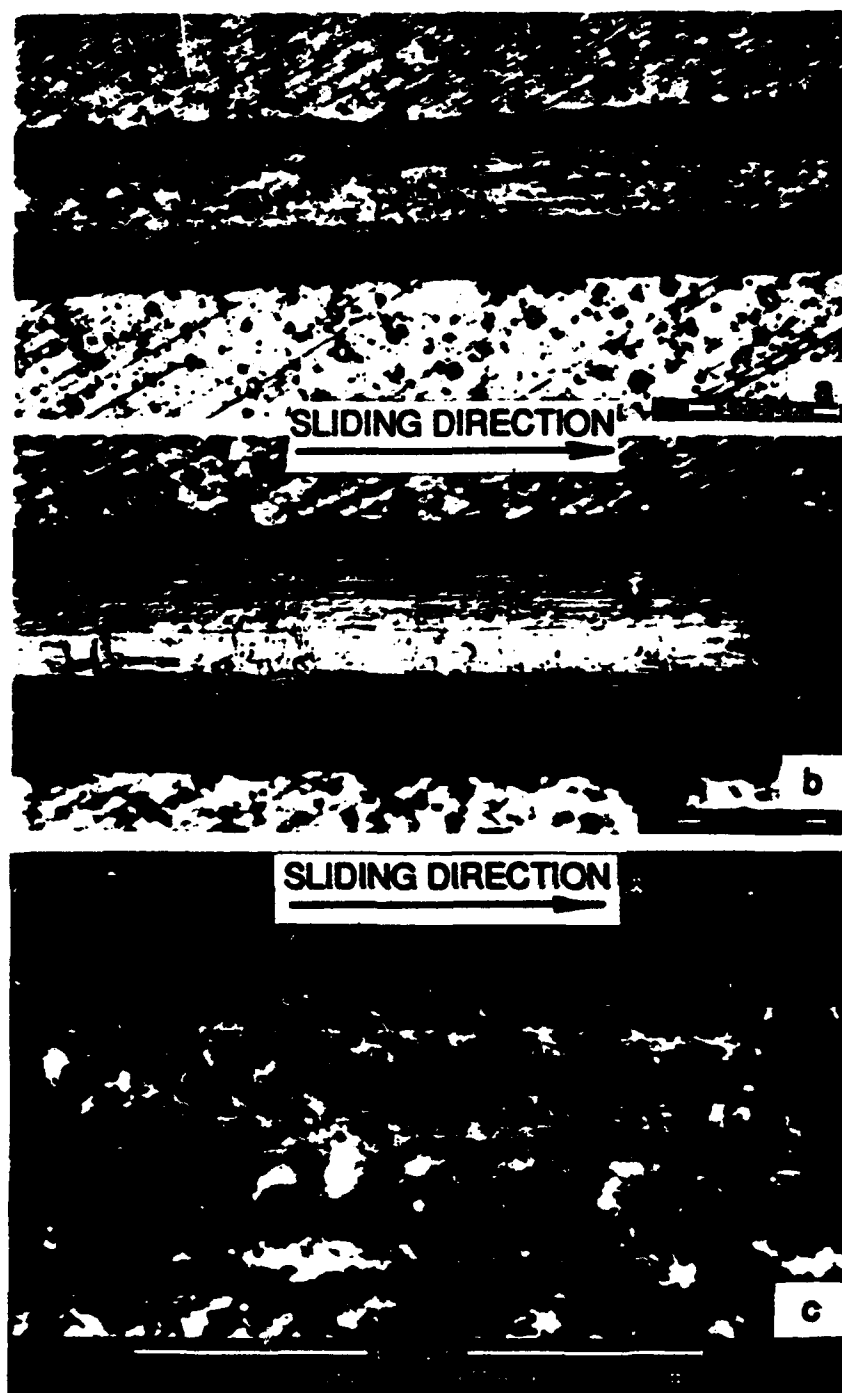


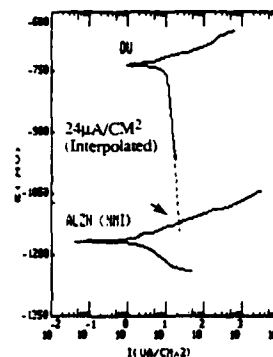
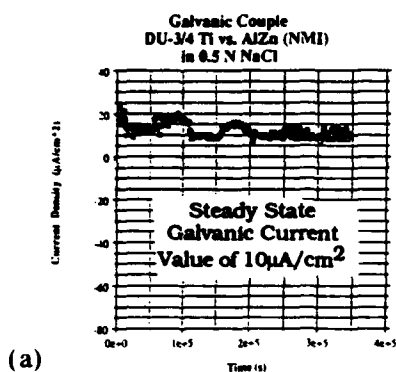
Fig. 3. (a), (b) Optical micrographs of a scratch corresponding to normal loads of (a) 42 N and (b) 79.2 N for multilayer TiN-Ti/TiN-coated DU-0.75Ti specimens. (c) SEM micrograph of the same scratch corresponding to a normal load of 55.6 N. (Magnifications: (a), (b) 200 $\times$ , (c) 750 $\times$ .)

### 3.2. Galvanic corrosion behavior

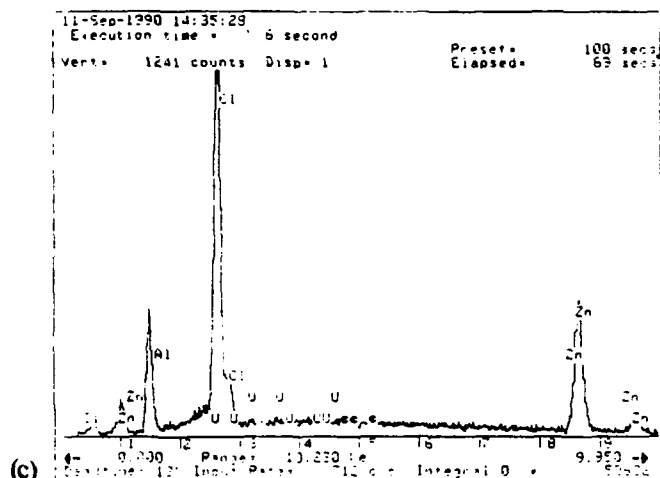
#### 3.2.1. (DU-0.75Ti) vs. (Al-Zn)-(coated DU-0.75Ti)

The current flow-time curve for this couple (Fig. 4(a)) falls in a relatively low current density range. The initial current density drop indicates oxide film formation on the anode; this is followed by a gradual rise as

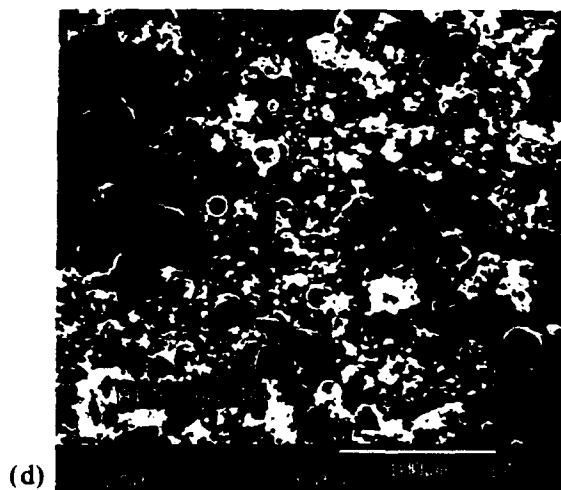
the oxide film was removed from the Al-Zn anode. Several cycles in current density followed before a steady state value of  $10 \mu\text{A cm}^{-2}$  (Table 2) was reached after immersion for 70 h ( $2.5 \times 10^5$  s) in the 0.5 N NaCl solution. The positive current density (Table 2) indicated that Al-Zn was anodic and DU-0.75Ti was



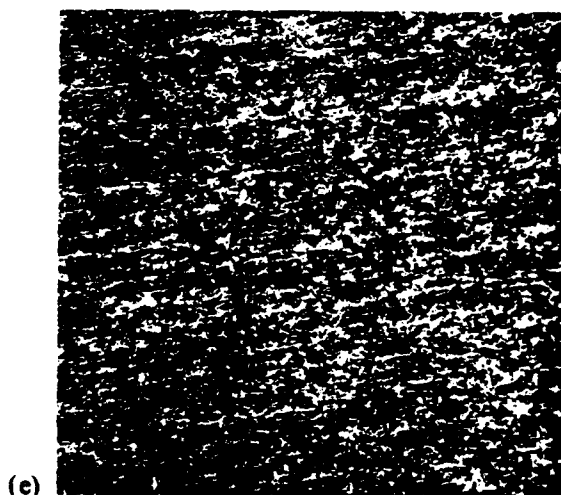
Depleted Uranium vs. AlZn (NMI) Coating  
Polarization scans in 0.5 N NaCl  
Scan rate 0.3 mV/s. No Purge



EDS of AlZn after test



SEM of AlZn after test



Optical micrograph of DU after test at  $50\times$  (against AlZn)

Fig. 4. Galvanic corrosion of (Al-Zn)-coated vs. uncoated DU-0.75Ti. (a) galvanic couple DU-0.75Ti vs. Al-Zn in 0.5 NaCl; (b) DU vs. Al-Zn in 0.5 N NaCl (scan rate,  $0.3 \text{ mV s}^{-1}$ ; no purge); (c) EDS of Al-Zn after test; (d) SEM micrograph of Al-Zn after test; (e) optical micrographs of DU after test (against Al-Zn). (Magnification: (e)  $50\times$ .)

TABLE 2.  $E_{\text{corr}}$ ,  $E_{\text{couple}}$  and current density from polarization scans, and current density from galvanic couple measurements

	$E_{\text{corr}}$ (mV (SCE))	$E_{\text{couple}}$ (mV (SCE))	Polarization current density ( $\mu\text{A cm}^{-2}$ )	Galvanic current density ( $\mu\text{A cm}^{-2}$ )
DU	–735			
DU vs. TiN-coated DU	–297 <sup>a</sup>	–720	–5	–10
DU vs. Al alloy 7075	–809 <sup>b</sup>	–796	12	10
DU vs. (Al–Zn)-coated DU	–1138 <sup>c</sup>	–1120	24	10

Positive current densities indicate that the DU is cathodic while negative values indicate that the DU is anodic for each couple.

<sup>a</sup> $E_{\text{corr}}$  for TiN-coated DU.

<sup>b</sup> $E_{\text{corr}}$  for aluminum alloy 7075.

<sup>c</sup> $E_{\text{corr}}$  for (Al–Zn)-coated DU.

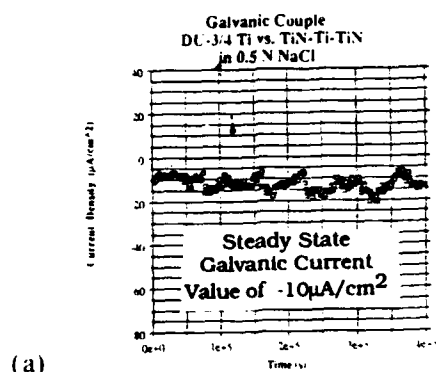
cathodic. Figure 4(b) shows the results of polarization measurements of Al–Zn as anode and DU–0.75Ti as cathode. The extrapolated intersection of the anodic and cathodic potentials represents the potential and the current density of the short-circuited galvanic couple. Table 2 compares the values of the corrosion potentials  $E_{\text{corr}}$  and the galvanic couple potential  $E_{\text{couple}}$  derived from these polarization scans. These data show that DU–0.75Ti is polarized significantly in the cathodic direction and behaves as cathode. On the contrary,  $E_{\text{couple}}$  for Al–Zn is slightly anodic to  $E_{\text{corr}}$ , suggesting that Al–Zn could support the anodic reaction. The anodic curve for Al–Zn intersects the extrapolated DU–0.75Ti cathodic curve along the oxygen reduction region where concentration polarization becomes important as the reduction rate approaches the limiting diffusion current density. A comparison of the measured galvanic current density and the current density extrapolated from anodic and cathodic polarization scans shows reasonable agreement (Table 2). Figure 4(d) is a scanning electron micrograph of the (Al–Zn)-coated DU–0.75Ti specimen after galvanic corrosion testing for 90 h in a 0.5 N NaCl solution. Also shown in Fig. 4(c) is the EDS scan of the corroded surfaces. The globular and mud-cracked corrosion products are mainly aluminum or zinc chloride compounds. There was no evidence of exposure of the underlying DU–0.75Ti alloy. The EDS concentrations of the unexposed Al–Zn alloy coating were 47 at.% Al and 53 at.% Zn which is in reasonable agreement with the original composition of the Al–Zn alloy target used in cathodic arc plasma PVD processing. Higher zinc evaporation rates makes the slight zinc enrichment of the coating an expected effect. Figure 4(e) shows the DU–0.75Ti member of the couple after the same exposure in chloride solution. There is very little evidence of corrosion indicative of the galvanic protection from the Al–Zn coating.

### 3.2.2. (DU–0.75Ti) vs. (Multilayer (TiN/Ti/TiN)-coated DU–0.75Ti)

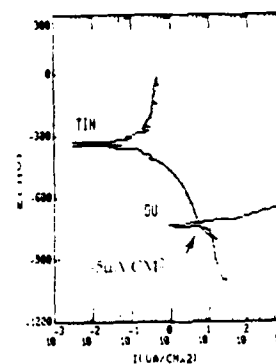
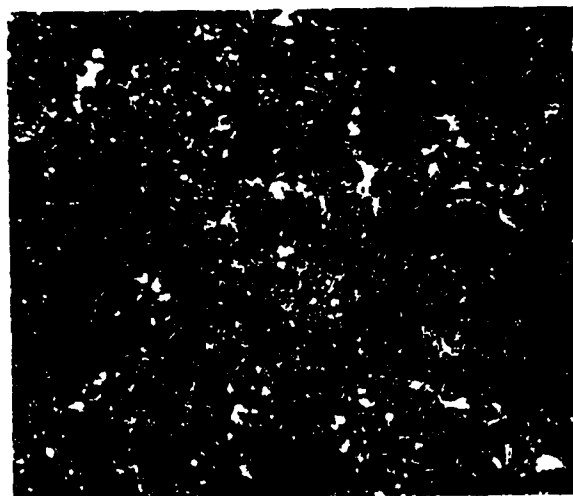
Figure 5(a) represents the current flow characteristics of this couple. The current density remained steady at  $-10 \mu\text{A cm}^{-2}$  for 15 h ( $5.4 \times 10^4$  s) before a series of falls and rises was observed until a pseudo-steady state value of  $-15 \mu\text{A cm}^{-2}$  was reached after exposure for about 110 h ( $3.9 \times 10^5$  s) to the chloride solution. The negative values shown in Table 2 indicated that the DU–0.75Ti alloy behaved as the anodic member of this couple.

Figure 5(b) contains polarization scans of DU–0.75Ti alloy as the anode and the coated alloy as cathode. A comparison of  $E_{\text{couple}}$  with  $E_{\text{corr}}$  of the uncoupled alloys (Table 2) revealed that DU–0.75Ti was polarized in the anodic direction and therefore behaved as anode. The (TiN/Ti/TiN)-coated alloy was significantly polarized in the cathodic direction indicative of cathodic behavior. The intersection of the anodic curve for DU–0.75Ti and the cathodic curve for the coated alloy occurs along the region of the limiting current density of oxygen reduction where concentration polarization becomes important. The good agreement between the measured galvanic current density and the current density extrapolated from the anodic and cathodic polarization scans is shown in Table 2.

Figures 5(c) and 5(d) contain micrographs of both the DU–0.75Ti alloy and the multilayered coated alloy surfaces (includes an EDS scan (Fig. 5(e)) after galvanic corrosion testing for 110 days in the chloride solution. The DU–0.75Ti alloy is completely covered with corrosion products indicative of relatively severe corrosion of this alloy. On the contrary the coated alloy is relatively corrosion free except for minor amounts of white corrosion products which appear to be chlorides. The silvery coating which is mainly titanium (see the EDS scan) appears to have some porosity and in these areas the EDS scan shows the presence of some DU.

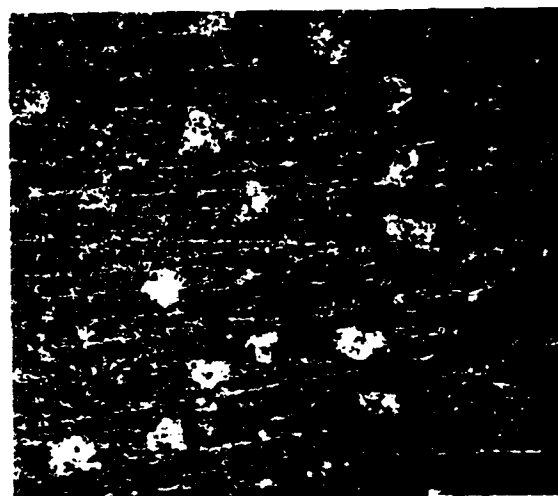


(a)

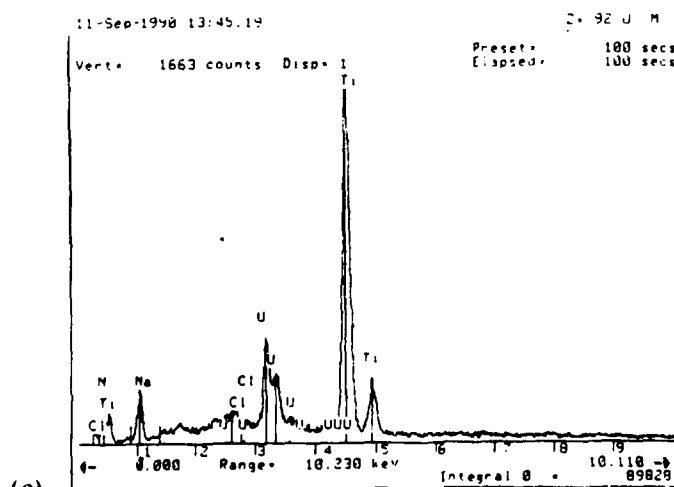
(b) Depleted Uranium vs. TiN-Ti-TiN Coating  
Polarization scans in 0.5 N NaCl  
Scan rate 0.3 mV/s. No Purge

(c)

Optical micrograph of DU after test at 50x



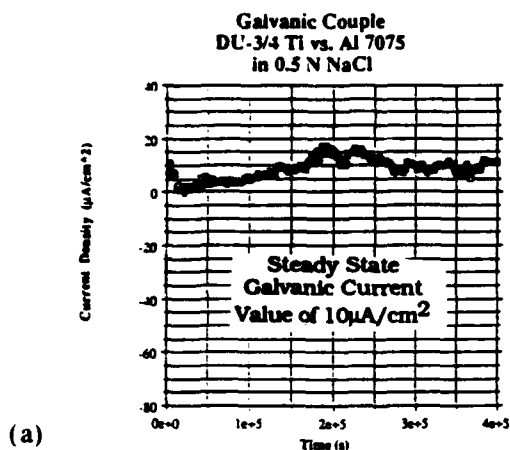
(d)

Optical micrograph of TiN-Ti-TiN  
coating after test at 50x

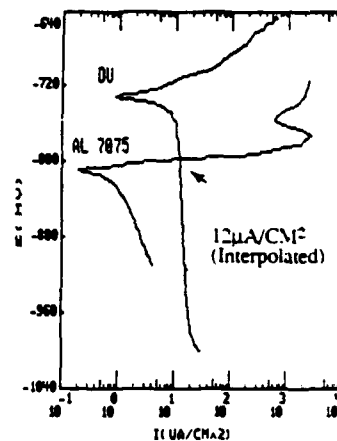
(e)

EDS of Ti-Ti-TiN after test (showing traces of Uranium)

Fig. 5. Galvanic corrosion of TiN/Ti-TiN-coated vs. uncoated DU-0.75Ti: (a) galvanic couple DU-0.75Ti vs. TiN-Ti-TiN in 0.5 N NaCl; (b) DU vs. TiN-Ti-TiN in 0.5 N NaCl (scan rate,  $0.3 \text{ mV s}^{-1}$ ; no purge); (c) optical micrograph of DU after test; (d) optical micrographs of TiN-Ti-TiN after test; (e) EDS of TiN-Ti-TiN after test (showing traces of uranium). (Magnification: (c), (d) 50x.)



(a)



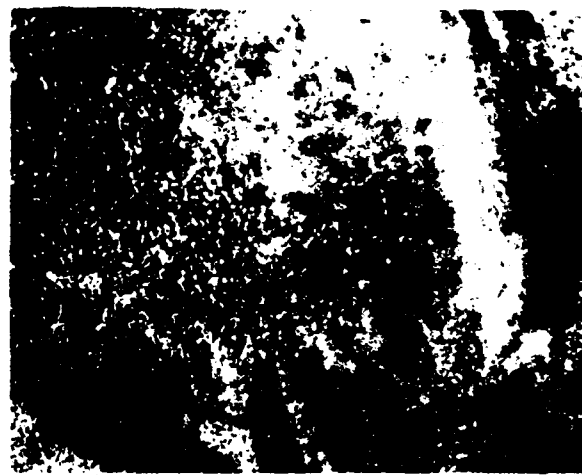
(b)

Depleted Uranium vs. Al 7075  
Polarization scans in 0.5 N NaCl  
Scan rate 0.3 mV/s, No Purge



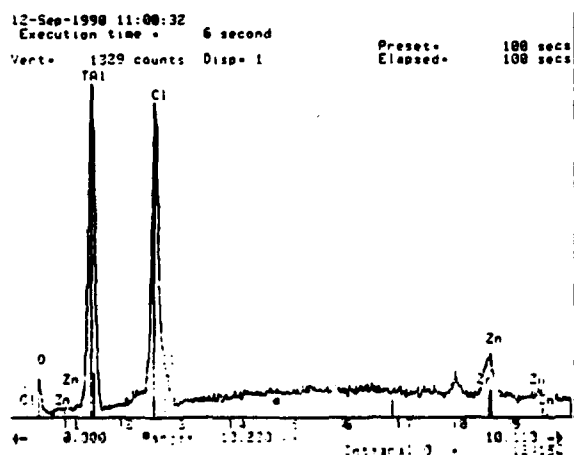
(c)

Optical micrograph of Al after test at  $60\times$



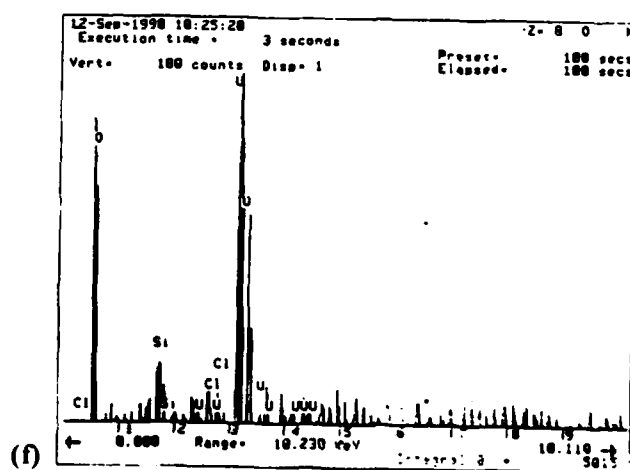
(d)

Optical micrograph of DU after test at  $10\times$



(e)

EDS of Al 7075 after test



(f)

EDS of DU after test

Fig. 6. Galvanic corrosion of aluminum alloy 7075 vs. uncoated DU-0.75Ti: (a) galvanic couple DU-0.75Ti vs. aluminum alloy 7075 in 0.5 N NaCl; (b) DU vs. aluminum alloy 7075 in 0.5 N NaCl (scan rate,  $0.3\text{ mV s}^{-1}$ ; no purge); (c) optical micrograph of aluminum alloy 7075 after test; (d) optical micrograph of DU after test; (e) EDS of aluminum alloy 7075 after test; (f) EDS of DU after test. (Magnification: (c)  $60\times$ ; (d)  $10\times$ .)

### 3.2.3. (DU–0.75Ti) vs. Al alloy 7075-T6

The galvanic current decreased initially to a very low (close to zero) value and then gradually increased to  $15 \mu\text{A cm}^{-2}$  (Fig. 6), later decreasing back to a steady state value of  $10 \mu\text{A cm}^{-2}$  after exposure for about 100 h ( $3.6 \times 10^5$  s). The fluctuations in current observed after exposure for 40 h ( $1.4 \times 10^5$  s) were probably due to pitting of the aluminum alloy 7075. The positive current density shown in Table 2 indicated that aluminum alloy 7075 was anodic to DU–0.75Ti. Polarization scans for aluminum alloy 7075 as anode and DU–0.75Ti as cathode are displayed in Fig. 6(b). A comparison of  $E_{\text{corr}}$  and  $E_{\text{couple}}$  derived from these scans (Table 2) shows that the DU–0.75Ti was not significantly polarized and the aluminum alloy 7075 was only slightly anodic to  $E_{\text{corr}}$ , which suggests that this alloy would support both cathodic and anodic reactions. The anodic curve for aluminum alloy 7075 intersects the DU–0.75Ti curve along the region of the limiting current density of oxygen reduction. Table 2 shows good agreement between the measured galvanic current density and the current density extrapolated from anodic and cathodic polarization scans. McIntyre *et al* [9] have also studied the (DU–0.75Ti)–Al alloy 7075-T6 couple for a 1:1 area ratio. They reported that the DU–0.75Ti behaved as the anode during the initial immersion for 72 h but, after 72 h, the current reversed and the DU–0.75Ti became the cathode. Therefore it is not surprising to see DU–0.75Ti behaving as either cathode or anode when coupled to aluminum alloy 7075-T6 depending upon the specific experimental conditions.

Figures 6(c)–6(f) contain micrographs and EDS scans of both members of the couple after exposure for 110 h to the chloride solutions. The aluminum

alloy exhibited severe pitting. Corrosion products present are in the main chlorides and oxides. The DU–0.75Ti exhibited only slight corrosion in the form of oxides with trace amounts or chlorides.

## 4. Conclusions

Al–Zn alloy coatings on DU–0.75Ti alloy specimens provide galvanic protection to the substrate and exhibit better mechanical strength than do multilayer TiN/Ti/TiN coatings which can be used only if they are defect-free. Aluminum alloy 7075-T6 can support both cathodic and anodic reactions, and therefore its ability to provide galvanic protection to DU–0.75Ti alloy is limited.

## References

1. F. Chang, M. Levy, B. Jackman and W. B. Nowak, *Surf. Coat. Technol.*, **39–40** (1989) 721–731.
2. T. Z. Kattamis, F. Chang and M. Levy, *Surf. Coat. Technol.*, **43–44** (1990) 390–401.
3. J. Ahn, K. L. Mittal and R. H. MacQueen, in K. L. Mittal (ed.), *Adhesion Measurement of Thin Films, Thick Films and Bulk Coatings*, ASTM Spec. Publ. 640, 1978, p. 134 (ASTM Philadelphia, PA).
4. A. J. Perry, P. Laeng and H. E. Hintermann, *Proc. 8th Int. Conf. on Chemical Vapor Deposition*, Electrochemical Society, Pennington, NJ, 1981, p. 475.
5. A. J. Perry, *Thin Solid Films*, **107** (1983) 167.
6. P. A. Steinmann, P. Laeng and H. E. Hintermann, *Mater. Technol.*, **13** (1985) 85.
7. K. J. Bhansali and T. Z. Kattamis, *Wear*, **141** (1990) 59.
8. P. A. Steinmann, Y. Tardy and H. E. Hintermann, *Thin Solid Films*, **154** (1987) 333.
9. J. F. McIntyre, E. P. Lefevre and K. A. Musselman, *Corrosion*, **44** (8) (1988) 502.

# DISTRIBUTION LIST

No. of Copies	To
1	Office of the Under Secretary of Defense for Research and Engineering, The Pentagon, Washington, DC 20301
	Commander, U.S. Army Laboratory Command, 2800 Powder Mill Road, Adelphi, MD 20783-1145
1	ATTN: AMSLC-IM-TL
1	AMSLC-CT
	DARPA, 1400 Wilson Boulevard, Arlington, VA 22209
1	ATTN: Director, Materials Science
	Commander, Defense Technical Information Center, Cameron Station, Building 5, 5010 Duke Street, Alexandria, VA 22304-6145
2	ATTN: DTIC-FDAC
1	MIAC/CINDAS, Purdue University, 2595 Yeager Road, West Lafayette, IN 47905
	Commander, Army Research Office, P.O. Box 12211, Research Triangle Park, NC 27709-2211
1	ATTN: Information Processing Office
1	Dr. E. Chen
1	Dr. R. Rebar
1	Director, Materials Science
	Commander, U.S. Army Materiel Command (AMC), 5001 Eisenhower Avenue, Alexandria, VA 22333
1	ATTN: AMCSCI
1	AMCPO-BD
1	Technical Library
	Commander, U.S. Army Materiel Systems Analysis Activity, Aberdeen Proving Ground, MD 21005
1	ATTN: AMXSY-MP, Director
	Commander, U.S. Army Missile Command, Redstone Scientific Information Center, Redstone Arsenal, AL 35898-5241
1	ATTN: Technical Library
	Commander, U.S. Army Armament Research, Development and Engineering Center, Picatinny Arsenal, NJ 07806-5000
3	ATTN: SMCAR-AET-M, Dr. B. Lakshminarayan
3	Mr. A. Daniels
2	Technical Library
	Commander, U.S. Army Tank-Automotive Command, Warren, MI 48397-5000
1	ATTN: AMSTA-ZSK
2	AMSTA-TSL, Technical Library
1	AMSTA-RCK
	Commander, U.S. Army Foreign Science and Technology Center, 220 7th Street, N.E., Charlottesville, VA 22901-5396
3	ATTN: AIFRTC, Applied Technologies Branch, Gerald Schlesinger
	Commander, U.S. Army Natick Research, Development and Engineering Center, Natick, MA 01760-5015
3	ATTN: George Dittmeier
	Commander, U.S. Army Aviation Systems Command, Aviation Research and Technology Activity, Aviation Applied Technology Directorate, Fort Eustis, VA 23604-5577
1	ATTN: SAVDL-E-MOS (AVSCOM)
1	SAVDL-EU-TAP
	Director, U.S. Army Ballistic Research Laboratory, Aberdeen Proving Ground, MD 21005
1	ATTN: Technical Library
	Director, Benet Weapons Laboratories, LCWCL, USA AMCCOM, Watervliet, NY 12189
1	ATTN: Technical Library

No. of Copies	To
	Naval Research Laboratory, Washington, DC 20375-5000
1	ATTN: Code 5830
1	Code 2627
1	Code 6310, Dr. E. McCafferty
1	Code 4675, Mr. B. D. Sartwell
	Chief of Naval Research, Arlington, VA 22217
1	ATTN: Code 471
1	Code 1131, Dr. A. J. Sedriks
1	Code 1131, Dr. S. Fishman
	Chief of Naval Research, Washington, DC 20350
1	ATTN: OP-987, Director
	Naval Surface Weapons Center, Silver Springs, MD 20910
1	ATTN: Dr. J. Tydings, Code R32
1	Dr. Sutula, Code R33
1	Dr. R. Lee, Code R34
	Commander, Naval Surface Weapons Center, Dahlgren, Laboratory, Dahlgren, VA 22448
1	ATTN: Dr. Bettadapur, Code C53
	Commander, Naval Civil Engineering Laboratory, Port Hueneme, CA 93043
1	ATTN: Dr. R. Dricko
1	Mr. D. Zarate
1	Mr. J. Jenkins
1	Mr. D. Brunner
	Commander, Naval Ocean Systems Center, San Diego, CA 92152
1	ATTN: Mr. Gordon Chase, Code 932
	Commander, Naval Air Development Center, Warminster, PA 18974
1	ATTN: Dr. V. S. Agarwala
	Naval Post Graduate School, Monterey, CA 93948
1	ATTN: Code 57BP, R. E. Ball
1	Technical Library
	NASA - Ames Research Center, Army Air Mobility Research and Development Laboratory, Mail Stop 207-5, Moffett Field, CA 94035
1	ATTN: SAVDL-AS-X, F. H. Immen
	NASA - Langley Research Center, Hampton, VA 23665-5225
1	ATTN: Technical Library
	NASA - Lewis Research Center, 21000 Brookpark Road, Cleveland, OH 44135-3191
1	ATTN: Technical Library
	IIT Research Institute, 10 West 35th Street, Chicago, IL 60616
1	ATTN: Director, Materials Research
	Commander, U.S. Air Force Materials Laboratory, Wright-Patterson Air Force Base, Dayton, OH 45433
1	ATTN: Code MLSA, Mr. F. Meyer
1	Technical Library
	U.S. Air Force Office of Scientific Research, Bolling Air Force Base, Washington, DC 20332
1	ATTN: Dr. A. Rosenstein
	National Institute of Standards and Technology, Gaithersburg, MD 20899
1	ATTN: Dr. N. E. Pugh
1	Dr. U. Bertocci
1	Dr. J. W. Martin
1	Dr. R. E. Ricker
1	Technical Library



No of Copies	To
1	Georgia Institute of Technology, Atlanta, GA 30332 ATTN: Library
1	Lukens Steel Company, Coatesville, PA 19320 ATTN: Director, R&D
1	Corpus Christi Army Depot, Corpus Christi, TX 78419 ATTN: Technical Library
1	Bethlehem Steel Corp., Research Laboratories, Bethlehem, PA 18016 ATTN: Dr. H. Townsend
1	VAC-TEC Systems, Inc., 6101 Lookout Road, Boulder, CO 80301 ATTN: Dr. P. C. Johnson, Vice President
1	Lawrence Livermore National Laboratory, P.O. Box 808, Livermore, CA 94550 ATTN: Dr. D. M. Sanders, L-332
1	Technical Library
1	Northeastern University, Electrical and Computer Engineering, Boston, MA 02115 ATTN: Dr. C. Chan
1	Prof. W. Nowak
1	Florida Atlantic University College of Engineering, Department of Ocean Engineering, P.O. Box 3091, Boca Raton, FL 33431-0991 ATTN: Prof. J. McIntyre
1	University of Illinois, Department of Materials Science and Engineering, Urbana, IL 61801 ATTN: Prof. J. M. Rigsbee
2	Director, U.S. Army Materials Technology Laboratory, Watertown, MA 02172-0001 ATTN: SLCMT-TML
7	Authors

U.S. Army Materials Technology Laboratory,  
Watertown, Massachusetts 02172-0001  
ADhesion and Corrosion Behavior of Al-Zn  
and TiN/Ti/TiN Coatings on a DU-0.75wt.%  
Ti Alloy - F. C. Chang, M. Levy, R. Huie,  
M. Kane, P. Buckley, T. Z. Kattamis, and  
G. R. Lakshminarayan

Technical Report MTL TR 92-56, August 1992, 12 pp -  
illus-tables

AD UNCLASSIFIED  
UNLIMITED DISTRIBUTION

Key Words  
Uranium alloys  
Uranium-titanium alloys  
Vapor deposition

Al-Zn alloy and multilayer TiN/Ti/TiN thin coatings were deposited on DU-0.75Ti alloy specimens by a cathodic arc plasma physical vapor deposition process. The quality, soundness and adhesion of the coatings to the substrate were evaluated by automatic scratch testing, in combination with optical and scanning electron microscopy examination of the scratch morphology. The galvanic corrosion behavior of DU-0.75Ti alloy coupled to the coated alloys and aluminum alloy 7075-T6 was also investigated by electrochemical tests in a 0.5 N NaCl aqueous solution.

U.S. Army Materials Technology Laboratory,  
Watertown, Massachusetts 02172-0001  
ADhesion and Corrosion Behavior of Al-Zn  
and TiN/Ti/TiN Coatings on a DU-0.75wt.%  
Ti Alloy - F. C. Chang, M. Levy, R. Huie,  
M. Kane, P. Buckley, T. Z. Kattamis, and  
G. R. Lakshminarayan

Technical Report MTL TR 92-56, August 1992, 12 pp -  
illus-tables

AD UNCLASSIFIED  
UNLIMITED DISTRIBUTION

Key Words  
Uranium alloys  
Uranium-titanium alloys  
Vapor deposition

Al-Zn alloy and multilayer TiN/Ti/TiN thin coatings were deposited on DU-0.75Ti alloy specimens by a cathodic arc plasma physical vapor deposition process. The quality, soundness and adhesion of the coatings to the substrate were evaluated by automatic scratch testing, in combination with optical and scanning electron microscopy examination of the scratch morphology. The galvanic corrosion behavior of DU-0.75Ti alloy coupled to the coated alloys and aluminum alloy 7075-T6 was also investigated by electrochemical tests in a 0.5 N NaCl aqueous solution.

U.S. Army Materials Technology Laboratory,  
Watertown, Massachusetts 02172-0001  
ADhesion and Corrosion Behavior of Al-Zn  
and TiN/Ti/TiN Coatings on a DU-0.75wt.%  
Ti Alloy - F. C. Chang, M. Levy, R. Huie,  
M. Kane, P. Buckley, T. Z. Kattamis, and  
G. R. Lakshminarayan

Technical Report MTL TR 92-56, August 1992, 12 pp -  
illus-tables

AD UNCLASSIFIED  
UNLIMITED DISTRIBUTION

Key Words  
Uranium alloys  
Uranium-titanium alloys  
Vapor deposition

Al-Zn alloy and multilayer TiN/Ti/TiN thin coatings were deposited on DU-0.75Ti alloy specimens by a cathodic arc plasma physical vapor deposition process. The quality, soundness and adhesion of the coatings to the substrate were evaluated by automatic scratch testing, in combination with optical and scanning electron microscopy examination of the scratch morphology. The galvanic corrosion behavior of DU-0.75Ti alloy coupled to the coated alloys and aluminum alloy 7075-T6 was also investigated by electrochemical tests in a 0.5 N NaCl aqueous solution.

U.S. Army Materials Technology Laboratory,  
Watertown, Massachusetts 02172-0001  
ADhesion and Corrosion Behavior of Al-Zn  
and TiN/Ti/TiN Coatings on a DU-0.75wt.%  
Ti Alloy - F. C. Chang, M. Levy, R. Huie,  
M. Kane, P. Buckley, T. Z. Kattamis, and  
G. R. Lakshminarayan

Technical Report MTL TR 92-56, August 1992, 12 pp -  
illus-tables

AD UNCLASSIFIED  
UNLIMITED DISTRIBUTION

Key Words  
Uranium alloys  
Uranium-titanium alloys  
Vapor deposition

Al-Zn alloy and multilayer TiN/Ti/TiN thin coatings were deposited on DU-0.75Ti alloy specimens by a cathodic arc plasma physical vapor deposition process. The quality, soundness and adhesion of the coatings to the substrate were evaluated by automatic scratch testing, in combination with optical and scanning electron microscopy examination of the scratch morphology. The galvanic corrosion behavior of DU-0.75Ti alloy coupled to the coated alloys and aluminum alloy 7075-T6 was also investigated by electrochemical tests in a 0.5 N NaCl aqueous solution.